

Accepted Manuscript

Morphology and strength of acrylonitrile butadiene styrene welds performed by robotic friction stir welding

N. Mendes, A. Loureiro, C. Martins, P. Neto, J.N. Pires

PII: S0261-3069(14)00579-2

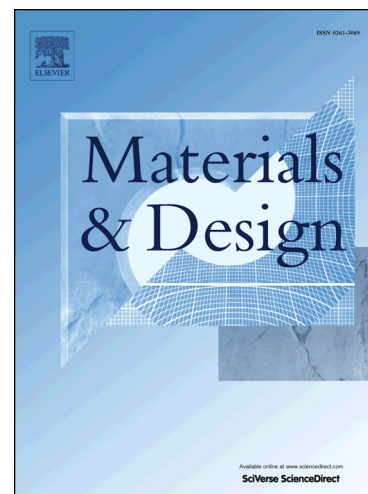
DOI: <http://dx.doi.org/10.1016/j.matdes.2014.07.047>

Reference: JMAD 6670

To appear in: *Materials and Design*

Received Date: 14 May 2014

Accepted Date: 14 July 2014



Please cite this article as: Mendes, N., Loureiro, A., Martins, C., Neto, P., Pires, J.N., Morphology and strength of acrylonitrile butadiene styrene welds performed by robotic friction stir welding, *Materials and Design* (2014), doi: <http://dx.doi.org/10.1016/j.matdes.2014.07.047>

This is a PDF file of an unedited manuscript that has been accepted for publication. As a service to our customers we are providing this early version of the manuscript. The manuscript will undergo copyediting, typesetting, and review of the resulting proof before it is published in its final form. Please note that during the production process errors may be discovered which could affect the content, and all legal disclaimers that apply to the journal pertain.

Morphology and strength of acrylonitrile butadiene styrene welds performed by robotic friction stir welding

N. Mendes^a, A. Loureiro^a, C. Martins^b, P. Neto^{a*}, J.N. Pires^a

nuno.mendes@dem.uc.pt, altino.loureiro@dem.uc.pt, cmartins@dep.uminho.pt, jnp@robotics.dem.uc.pt

^aCEMUC - Universidade de Coimbra, Rua Luís Reis Santos, 3030-788 Coimbra, Portugal

^bIPC/I3N - Universidade do Minho, Campus de Azurém, 4800-058 Guimarães, Portugal

*Corresponding author: Tel.: +351239790700; fax: +351239790701. E-mail address:

pedro.neto@dem.uc.pt

Abstract:

The aim of this study is to examine the main factors affecting friction stir welding (FSW) of acrylonitrile butadiene styrene (ABS) plates, performed by a robotic system developed to this purpose. Welds were carried out using a tool with stationary shoulder and an external heating system. The welding parameters studied were the axial force, rotational and traverse speeds and temperature of the tool. The major novelty is to perform FSW of a polymer in a robotic system and to study the influence of the axial force on weld quality. In a robotic solution the control of axial force allows to eliminate robot positional errors and guarantee the contact between the FSW tool and the work pieces. Strength and strain properties of the welds are evaluated and correlated with the morphology of the welded zone. A comparison between welds produced in the robotic FSW system and in a dedicated FSW machine is presented. It is shown the feasibility of robotic FSW of ABS without deteriorating the mechanical properties of the welds in relation to those produced in the dedicated FSW machine.

Keywords: Robotic Friction Stir Welding; Acrylonitrile butadiene styrene; Stationary shoulder tool; Weld defects; Mechanical properties.

1. Introduction

FSW of polymers is an attractive welding process due to the characteristics conferred to the welds. Strand [1] compared the most common welding processes used to join polymers, concluding that FSW is the process where it is achieved higher weld strength efficiency. This process enables the production of

highly efficient welded seams with low energy consumption. In addition, relatively low cost is implied, because of its low use of energy, and it does not require the addition of filler materials. Furthermore, FSW does not require skilled professionals, and can be easily automated. The traditional FSW process is illustrated in Fig. 1. Nelson et al. [2] claimed that the traditional FSW tools do not give proper results in terms of weld morphology and tensile strength when applied to polymeric materials. This effect is caused by specific properties of polymeric materials, such as their low melting temperature and low thermal conductivity when compared to metals. In order to overcome these difficulties, several FSW tools with different geometries have been developed. One such example is that created by Strand [3], called hot shoe, which consists of a rotating pin and a static shoe heated by electrical resistances. This author pointed out good results obtained in some welds, in spite of the fact that some welds have presented poor surface finish and few voids. On the other hand, Kiss and Czigány [4] succeeded in joining polypropylene (PP) sheets by FSW using conventional milling tools, rotating in the opposite direction to that of milling operations. However, the mechanical properties of the welded seams were poor. Scialpi et al. [5] presented a new concept of FSW tool: the vibrblade welding tool consisting of a vibrating blade connected to a vibrating shoe. During the welding process the blade vibrates inside the weld joint while the shoe moves in contact with the upper surface of the weld joint. Although the results of this technique were very good, it presented several drawbacks because of the complexity of the mechanism required to operate the tool, and the short working life of the blade, as concluded by Scialpi et al. [6]. Furthermore, this tool only could be used in welding joints of linear trajectory.

Aydin [7] developed a FSW tool with a larger shoulder, compared to the traditional FSW tool used to weld metallic materials, and a heating system placed at the root of the seam which enables the production of defect-free welds with a basin-like nugget zone. However, the weld crown surface was very rough, with non-aesthetic surface. The same tool concept without heating system has been used in other studies, which are presented below [8–12], to investigate the influence of some welding parameters in welded seams quality. The main drawback in the welded seams produced along these studies, as well as in the study carried out by Aydin [7], was bad surface quality of the welds. Bozkurt [8] studied the influence of FSW parameters: rotational speed, traversing speed and tilt angle on high density polyethylene (HDPE) plates. It was concluded that rotational speed is the most influent parameter in the seam quality while tilt angle is the least influent parameter. Payganeh et al. [9] studied the influence of the same parameter investigated by Bozkurt [8] and also the pin tool geometry on a polypropylene (PP) composite with 30%

glass fibre. It is reported that a taper pin with groove provides better results than other pin shapes. Furthermore, it is shown that larger rotational speed, lower traverse speed and larger tilt angle allows to reach better quality welds. Arici and Sinmazçelýk [10] showed that defects on the seam root can be eliminated by double passes of tool on FSW of medium density polyethylene (MDPE). The influence of the pin geometry in traversing force (F_x in Fig. 1) generated by FSW of PP plates was studied in Panneerselvam and Lenin [11]. The same authors [12] studied the influence of thread direction of the pin in FSW quality of nylon 6. This study concluded that the best seams are obtained when the FSW tool drives material flow towards seam root. These results confirm previous studies presented in Nelson et al. [2]. Kiss and Czigány [13] have proposed the use of a static shoe connected with the milling tool (similar to the hot shoe tool). This new tool has demonstrated promising results, the best welds performed in PP and polyethylene terephthalate glycol (PETG) displayed about 90 (%) of tensile strength observed in the base material. The tool rotational speed has shown to be the most important parameter in the FSW of PP sheets as shown by Kiss and Czigány [14]. Although other parameters such as tool geometry and size, traverse speed, warming temperature and dwell time also play an important role, as they contribute to heat generation and material flow in the stir zone. Bagheri et al. [15] have studied the influence of welding parameters rotational speed, traverse speed and shoulder temperature at the beginning of the FSW process. A hot shoe tool was used in this study and the good results allowed by this tool were observed once more. However, quality welds are only reported at low traverse speed values. A recent study proposed by Pirizadeh et al. [16] presented a new concept of FSW tool named self-reacting friction stir welding (SRFSW). This tool consists of two non-rotational opposing shoulders on the crown and root sides of the joint. It was studied the influence of the process parameters tool rotational speed, tool translational speed and shape of the pin. In spite of the fact that the authors have reported good results (high weld tensile strength), they are worse than the results presented by other studies [15,17]. This is likely because the design of the FSW tool that prevents the tool operates at high rotational speed and generates enough heat to promote a strong bond.

Kiss and Czigány [13] proposed a K factor depending on the rotational speed, traverse speed and tool diameter as a key condition for obtaining good quality welds. The K factor should range from 150 to 400, with each parameter ranging inside maximum and minimum operational limits. However, the K factor does not account for the effect of external heating or the axial force, a parameter which greatly influences the formation of defects. Mendes et al. [17] proved that increasing the tool plunge axial force (F_z in Fig.

1) in FSW of ABS the weld defect size is reduced or removed and mechanical properties are improved. In fact, none of the previous studies use a robot to perform FSW of polymers and just Mendes et al. [17] present a preliminary study of the influence of axial force on the resultant welds. The use of anthropomorphic industrial robots in the FSW process can reduce the costs associated to this welding process and increase its flexibility. However, anthropomorphic industrial robots when submitted to high loads tend to present positional errors due to several factors:

- Low stiffness associated to its articulated structure;
- Vibrations due to robot structure and rotation of the tool;
- Positional error associated to the off-line programming process.

These kinds of difficulties are pointed out by Schneider et al. [18] and Leali et al. [19] in robotic machining, a manufacturing process that also requires high load capability. In this context, it is expected that the use of an industrial robot to perform FSW will require high load capabilities to produce quality welds. The majority of the published studies about FSW of polymers have been carried out in conventional milling machines that are robust machines and no positional or vibration difficulties arise.

In robotic welding systems, the axial force must be minimized due to the size and cost of robots as it increases with their payload. This axial force can be reduced by increasing the heat generated in the process, adjusting tool rotational speed, and/or adding external heat. The authors did not find any study in literature making mention to the application of anthropomorphic robots with low bearing capacity performing FSW in polymers.

This paper studies the influence of welding parameters on the microstructure and mechanical properties of welds produced in a robotic system. The welding parameters analysed are axial force, rotational speed and traverse speed. Furthermore, the influence of tool temperature in weld crown appearance is also analysed. The presented welds were performed in a robotic system which may introduce some perturbations in the FSW process due to the reduced stiffness of the mechanical structure of an anthropomorphic robot when it operates with relatively high contact forces. Because of that, robotic welds were compared with welds performed in a conventional FSW machine [17], in order to analyse the influence on the weld quality of the robotic system developed.

2. Materials and methods

Square butt welds were produced between ABS plates of 300×80×6 (mm³). Some characteristics of the material are presented in Table 1. ABS is a light material with low glass transition temperature, which has a broad spectrum of applications such as in the chemical and automobile industries.

A FSW tool consisting of a stationary shoulder and a conical threaded pin of 5.9 (mm) length and 10 (mm) and 6 (mm) in diameter, at the base and at the tip of the pin respectively, was developed to perform the welds (Fig. 2). A long stationary shoulder was designed in order to allow heating in front of and behind the pin. The shape of the shoulder is approximately rectangular with a hole in its centre (pin hole). The external dimensions of the shoulder are: 177 (mm) × 25 (mm) and its area is approximately 4396.7 (mm²). An anvil made of steel (ST 37) was used to fix and contain melted polymer in bottom surface of the welding joint.

The welding parameters studied were rotational speed, which varied between 1000 and 1500 (rpm), traverse speed (between 50 and 200 (mm/min)), and the axial force (between 1 and 2 (kN)). The selection of these parameters was based on previous tests. Henceforth the welds are designated according to the following convention: letter R followed by rotational speed in (rpm); letter T followed by traverse speed in (mm/min); and letter F followed by the axial force in (kN). Therefore, the designation R1500T100F2 corresponds to a weld carried out with a rotational speed of 1500 (rpm), a traverse speed of 100 (mm/min) and axial force of 2 (kN). All the welds were performed in a robotic FSW system composed by a robot Motoman ES 165N and an in-house FSW system developed for this effect, that allows the registration of welding data during tests, as described by Mendes et al. [20].

Although pressure is a more representative welding parameter than force, it was decided to identify the weld in relation to force. This is because pressure and force parameters are intrinsically related and the majority of the FSW equipment is parameterized by the force parameter and not pressure. In this study, the relation between pressure (P) and force (F) is given by:

$$P = \frac{F}{A_{\text{shoulder}} + A_{\text{pin cross section}}} = \frac{F}{4425 \text{ (mm}^2\text{)}} \quad (1)$$

Where, A_{shoulder} is the area of the shoulder and $A_{\text{pin cross section}}$ is the area of the pin cross section at the base of the pin.

The procedure of welding consists in penetrating the FSW tool in the welding joint controlling the robotic system in positional control. In order to suppress positional errors of the robot, the FSW tool penetrates in the welding joint till the desired contact force (value of the parameter force for each weld experiment) is reached. After a Dwell time of 10 (s) the robot starts moving in the longitudinal movement, where the

molten material is transferred from the leading edge to the trailing edge of the tool. During this movement the robotic system produce positional adjustments (axial penetration) controlled by a hybrid force/motion controller in order to keep the desired contact force [21]. Regarding to the heating system, the tool initially at room temperature 25 (°C) is heated during 20 (s) and let to stabilize the temperature of the tool (until the temperature starts decrease). After that, the heating system is turned on for periods of time of 3 (s) followed by a variable period of time where the temperature of the tool is stabilized. This procedure is repeated until the temperature of the tool is above 115 (°C). This procedure is performed initially (before starting welding) and during welding process. The reasons for this procedure are pointed out in section 3.

For the morphological analysis of the welds, samples were cut out of the weld seams into 10 (µm) thick sections, using a Leitz microtome at room temperature, equipped with a perpendicular slicing glass knife. Optical transmission microscopic analyses were conducted using an Olympus BH transmittance microscope, with digital camera Leica DFC280 and software Leica application suite - LAS V4.

For mechanical tests a minimum of five tensile specimens were removed from each weld, transversely to the welding direction, and tested in a 10 (kN) universal testing machine, SHIMADZU AG-X, at room temperature, according to the **ASTM: D638** standard. The samples were submitted to surface smoothing by milling in order to homogenise the thickness of the samples across the gauge section and eliminate any defect on the crown and root of the welds. The local strains were also determined by digital image correlation (DIC) using an Aramis 3D 5M optical system (GOM GmbH). Before testing, the specimens were prepared by applying a black speckle pattern randomly over the surface of the transverse samples previously painted mat white in order to enable data acquisition by DIC.

The hardness testing methodology used to assess the effectiveness of the welds was based on the procedure detailed in [22], which presents some microhardness analysis for different polymers. This choice is due to the inexistence of a standard for Vickers microhardness of polymers. The Vickers hardness of the surface was determined with a microhardness tester (durometer ZHU 0.2 Zwick-Roell) using a Vickers diamond indenter and a 200 (g) load applied for 15 seconds. Vickers hardness measurements were made in a sequential pattern, starting on the retreating side, going through the weld nugget and finishing on the advancing side. The minimum distance between measurements is of at least 1 (mm).

3. Results

3.1. Morphological and micrographic analyses

The weld crown surface is largely influenced by the tool temperature as shown by the three weld experiments illustrated in Fig. 3. The average temperature was 90 (°C) for the first experiment (R1500T60F1, Fig. 3(a)), 115 (°C) for the second experiment (R1000T200F1, Fig. 3(b)) and 130(°C) for the third experiment (R1500T50F1, Fig. 3(b)). The average temperature of each experiment ranges plus or minus 5 (°C). The weld crown of the first (90 (°C)) and the third (130 (°C)) experiments present some defect while the weld crown of the second (115 (°C)) experiment is practically free of defects.

The axial force has also a clear influence on the weld crown surface as well as on morphology through the thickness direction, as shown in Fig. 4 and Fig. 5, respectively. The weld produced with lower axial force (R1000T50F1) presents external and internal defects as shown in Fig. 4(a) and Fig. 5(a), respectively. The major external defect is a gap on the surface on the retreating side of the weld. This gap extends along the whole length of the weld as well as through the thickness (internal defects) of the weld. This internal defect is composed of cavities and pores on the border (stirring zone/thermo-mechanical affect zone) of the retreating side of the weld. The stirring zone is the region of the weld where melted/softened material is dragged by the FSW tool. The thermo-mechanical affect zone is the portion of polymeric material that undergoes some deformation due to heating and/or force applied by the FSW tool. Fig. 5(a) shows a weld with poor joining on the retreating side. The other two welds (R1000T50F1.5 and R1000T50F2) do not present visible external or internal defects as shown in Fig. 4(b) and (c) and Fig. 5(b) and (c), respectively. However, in these two welds is visible plastic deformation of polymeric material on the surface in the advancing side, see Fig. 4(b) and Fig. 4(c). The deformation on surface, which it is not considered a defect, occurs mainly on the advancing side because the polymeric material is more heated and softened on the advancing side than on retreating side [23]. Additionally, higher axial force promotes weld surface deformation by the pressure imposed to the softened material. The superficial deformation was not observed on the weld R1000T50F1 because this weld was performed at the lowest axial force, less energy is introduced into the weld and the stirred material is less softened. High compression (axial force) promotes the squeeze of the softened polymer which prevents the introduction of air into the weld and helps the cooling of the weld. Thus, shrinkage and void formation is prevented. On the other hand, high axial load increases the energy applied on the weld, leading to low cooling rate which is beneficial to weld quality (from a structural point of view and visual appearance).

Three welding conditions, R1000T100F1, R1250T100F1, R1500T100F1, were chosen to assess the influence of the tool rotational speed on weld quality. Fig. 6 shows the crown surface for the three welds and Fig. 7 shows their morphology through the thickness. While the welds R1250T100F1 and R1500T100F1, performed respectively with 1250 and 1500 (rpm), present excellent crown surface, Fig. 6(b) and Fig. 6(c) respectively, the weld carried out with 1000 (rpm) (R1000T100F1) presents pores and cavities on the retreating side, as shown in Fig. 6(a). Similar conclusions can be drawn by the analysis of the weld morphology through the thickness. The welds R1250T100F1 and R1500T100F1 present morphologies free of visible defects, while the weld R1000T100F1 presents lots of cavities, pores and voids on the border of the retreating side. In other words, with the increase of the rotational speed, the number of cavities on the retreating side decreased or disappeared. These defects suggest that the heat generated on the retreating side of the weld R1000T100F1 was insufficient to promote bonding of material plastically deformed to the base material. Therefore the tool rotational speed plays an important role in heat generation, as claimed by several authors, either in metals [24,25] or in polymers [7]. The concentration of defects on the retreating side is mainly related with lower heat generated on this side, as mentioned above. In fact, Heurtier et al. [24] pointed out that the material flow on the retreating and advancing sides are different and this is the main reason for the concentration of defects on the retreating side.

The effect of traverse speed on weld quality was analysed in welds R1250T50F2, R1250T100F2 and R1250T200F2, performed with traverse speeds of 50, 100 and 200 (mm/min), respectively. The welds R1250T100F2 and R1250T200F2 made with the highest traverse speeds, present excellent superficial finishing, with very smooth surface and without visible defects, see Fig. 8(b) and Fig. 8(c), unlike the weld R1250T50F2, Fig. 8(a), presents surface deformation and burnt material on the crown surface on the advancing side. This effect is likely caused by excessive heat input. In a previous study [17], where the welds were performed in a FSW machine, this phenomenon (burnt material) was not observed because the heat involved in the process was just generated by the friction between FSW tool and polymeric material. On the other hand, the welds presented in the current study were performed in the robotic system where the heat involved in the process beyond it is generated by the friction between FSW tool and polymeric material it is also transferred from the external heating system to the surface of the weld. This means that in the latter welds the heat input is higher than in the former welds. The welds R1250T50F2, R1250T100F2 and R1250T200F2 present ratios of rotational to traverse speeds (R (rpm)/ T

(mm/min)) of 25, 12.5 and 6.25, respectively. Although the dimension of the R/T ratio (1/mm) can seem non-understandable, the physical phenomenon can make this clearer. As shown above the rotational speed has a great influence in the energy generated in the welding process, thus, the rotational speed can be considered, in some way, as energy. On the other hand, the traverse speed can be understood as a conduction rate of that energy to the polymer. It can be concluded that the higher the R/T ratio, the higher the heat introduced into the weld. Thus, the R/T ratio of 25 on weld R1250T50F2 can be considered too high because it is visible some degradation on the weld surface, as shown in Fig. 8(a) where some scratches are visible. Taking into account all the welds shown above it can be stated that to obtain good weld crown appearance, the R/T ratio must be inferior to 20, when the FSW tool temperature is maintained at 115 (°C). The R/T ratio of 20 is obtained for the weld R1000T50F2, which displays good quality, as confirmed by the Fig. 4(c) and Fig. 5(c).

The weld R1250T200F2 that presents the best crown surface, actually, has the worst morphology through the thickness, see Fig. 8(c) and Fig. 9(c). This weld presents a lot of voids on the nugget and retreating side as well as poor mixing of polymeric material on retreating side. The morphology through the thickness of the other two welds, R1250T50F2 and R1250T100F2, do not present visible defects as shown on Fig. 9(a) and Fig. 9(b) respectively. Thus, the traverse speed plays also an important role in the weld quality. The R/T ratio can be used to define a threshold above which good quality welds is obtained. In the present investigation the R/T ratio must be higher than 10 in order to obtain welds with good crown appearance and free of internal defects, as confirmed by the weld R1000T100F1 (Fig. 6(a) and Fig. 7(a)). The current authors reached similar conclusions in a previous study on welds performed on a FSW machine [17]. It should be mentioned that all the welds suffer of lack of penetration (Fig. 5, Fig. 7 and Fig. 9), the pin was not enough long to avoid root defects. Although the use of force control, the control of the robotic system can cause tool displacements in the axial direction, the size of the root weld defects was approximately constant (this is not well mirrored by Fig. 5, Fig. 6 and Fig. 7). This topic is not approached in this study, however, it was approached by Arici and Sinmazçelýk [10], who proposed the use of double pass to eliminate root weld defects.

3.2. Mechanical performance

The weld quality was also assessed by the ultimate tensile strength and strain at break. In all welds studied, the fracture occurred on the retreating side of the weld. It was observed that there is a general

trend of weld tensile strength increase with increasing axial force, as shown in Fig. 10(a). This relation is particularly visible between the welds produced with axial force of 1 (kN) and 1.5 (kN). The tensile strength of the welds shown in Fig. 4 and Fig. 5 are represented in Fig. 10(a) by the R1000T50 curve. In this case, it is clearly visible the increase of tensile strength with increasing axial force. The weld R1000T50F1 presents the lowest tensile strength among the three weld conditions shown in Fig. 4 (R1000T50F1, R1000T50F1.5 and R1000T50F2). This behaviour is easily understood by the presence of defects on surface and retreating side of the weld R1000T50F1, Fig. 4(a) and Fig 5(a).

As can be seen by the analysis of Fig. 10(a), the parameter axial force has a high influence on the tensile strength of the welds, mainly on the welds where less heat is generated i.e. rotational speeds are lower than 1500 (rpm). This suggests that axial force promotes reduction of the pores and voids in the weld through the thickness direction. Higher axial force promotes removal of internal weld shrinkage or dragging air into the weld, which are the main causes pointed out in the literature [26] in the formation of defects (as voids) in FSW of polymers.

Fig. 10(b) shows that the welds produced at 1 (kN) present the lowest strain followed by the welds produced at 2 (kN) which are preceded by the welds produced at 1.5 (kN). This order of magnitude for the strain can be explained by the size of the zone of poor mixing of material, which is highlighted by an arrow in Fig. 5(a), Fig. 5(c) and Fig. 5(b), respectively. These figures allow to conclude that the larger the zone of poor mixing of material, the lower the strain of the weld.

The parameters rotational speed and axial force have similar influence on tensile strength and strain at break of welds. Fig. 11(a) shows that there is a general trend of increase tensile strength of welds with the increase of rotational speed. For instance, the tensile strength of the welds shown in Fig. 6 and Fig. 7 are represented in Fig. 11(a) by the T100F1 curve. In this case, it is visible the increase in tensile strength with the increase of rotational speed. This result is explained by the decrease of defects that act as stress concentrators. The welding parameter rotational speed provides an effect on strain similar to the effect on tensile strength, Fig. 11(b). This means that there is a tendency of increasing strain with increase of rotational speed.

It would be reckless to make any conclusion about the influence of traverse speed on tensile strength of the welds based on just some particular welding conditions. Although Bagheri et al. [15] have stated that high travel speed decreases the tensile strength, in the current study and in the study carried out by Sorensen et al. [27] seems to be excessive to make such statement. Actually, as can be seen in Fig. 12(a)

in some welding condition the statement of Bagheri et al. [15] is partially verified, for example R1000F1.5 and R1250F1.5, but the other welding conditions do not reflect this effect. Unlike in the case of the welds R1000F1 and R1250F1 the opposite effect is verified.

The increase of the traverse speed leads to decreasing weld strain, as shown in Fig. 12(b). This generalisation may perhaps be justified by the different morphologies presented by the welds. The weld morphologies presented in Fig. 9 display different flow lines as observed by Strand [3], who stated that low traverse speed results in less severe flow lines, onion ring, and retreating interface. Higher traverse speeds lead to more forced material flow, which in turn prevents the mixing of material. Thus, adhesion of polymeric material on the retreating side is lower and formation of defects in this zone is promoted, as exhibited by the weld R1250T200F2 (Fig. 9(c)).

The complete spectrum of mechanical properties of welds performed in the robotic system using heated tool at 115 (°C) is presented in Table 2. The best welds present high tensile strength and reasonable strain. The weld R1500T200F2 presents the best strength efficiency, 75.5 (%). The strength efficiency is the ratio between tensile strength of the welds and base material. The weld R1500T100F1.5 presents the best strain 9.2 (%) while base material presents 50 (%). Analysing Table 2, it can be stated that high tensile strength and strain performances are reached when high rotational speed and axial force are used to produce welds.

Hardness measurement can be used to estimate relative mechanical strength of welds in metallic materials. The weld R1500T100F200 was chosen to illustrate the hardness profile measured on the cross section because it presents no morphological defects. Defects can alter the results of hardness measurement. As shown in Fig. 13, the welding hardness is unchanged in relation to the hardness of base material, about 11 (HV0.2). Consequently, hardness does not give useful information about mechanical strength of welds in ABS.

4. Discussion

4.1. Temperature

Welds with good quality must display a smooth crown without any pores or cracks, because this kind of defects is usually the main reason for fracture initiation in polymeric welds, as stated by Frassine et al. [28], who have studied the resistance to crack initiation and propagation in the fracture of polymers.

The parameter tool temperature plays an important role in FSW of polymers. As shown by the Fig. 3(a), an average tool temperature of 90 (°C) provides poor weld crown appearance, where there is some porosity and formation of flash on the retreating side of the weld. In addition, the whole weld crown is rough, which means that the stirred material does not melt enough. Thus, when the cooling stage occurs, consolidation of material appears to be poor. It can be stated that to perform welds with smooth crown the tool temperature must be higher than 90 (°C). On the other hand, an average tool temperature of 130 (°C) also provides poor weld crown appearance, Fig. 3(c). In this experiment the weld crown and the thermo-mechanical affected zone on the surface (zone not stirred but affect by the temperature and pressure imposed by the shoulder) are burnt. This shows that the tool temperature of 130 (°C) is too high to perform FSW on ABS. However, high tool temperature is required to promote material mixing which explain the smoothness present in part of this weld crown. A similar effect have been reported by Bagheri et al. [15] when the initial tool temperature, before starts the welding process, assumes high values, the weld crown is burnt. It should be highlighted that while these authors only considered the tool temperature before start FSW process, the current study takes into account the tool temperature before and during the FSW process. Finally, an average tool temperature of 115 (°C) provides a quality weld crown, as shown in Fig. 3(b). The weld crown performed at 115 (°C) is smooth and free of pores. A tool temperature close the glass transition temperature of the polymer seems to be the most suitable to perform FSW.

Owing to low thermal conductivity of ABS, an increase in temperature of the tool does not imply an increase in stirred material temperature. Thus, the material that is in the interface shoulder/joint will be more affected by the tool temperature. In addition, the heat transferred between FSW tool and material occurs mainly by the shoulder than by the pin due to the fact that the shoulder area is larger. However, the pin plays an important role in the generation of heat by friction. It is expectable that the anvil has low influence on the weld quality, particularly at the root of the weld. This statement is based on the fact that ABS is a bad thermal conductor and the used anvil has a large volume that enables heat spreading for the whole anvil preventing that it reaches a level of temperature capable to cause any influence on the weld quality. It was found that higher values of rotational speed and lower values of traverse speed, without supplying external heating, promote increasing of tool temperature and consequently increasing weld crown temperature too. This increase in temperature is due to friction generated inside the FSW tool (tool mechanism) and friction generated between the pin of the tool and polymeric material. Since polymeric

material is low thermal conductor, heat generated between pin and material tends to flow through the pin to the shoulder which in turn makes heat to flow/spread to the weld surface. In some welding conditions, it was found that external heating is not required because the welding process generates enough heat by friction. Moreover, in some other welding conditions without supplying external heating it is generated too much heat, leading to burnt of weld crown surface. This suggests that the use of a cooling system could improve weld quality.

Owing to the similarity of the welding parameters and material approached in this study and the ones approached by Mendes et al. [17] in a previous research, the results of both studies are compared below. In the previous study the welds were done in a FSW machine, without using any external heating. Robotic welds present in general smoother crown surface and better morphology through the thickness than the welds performed in the FSW machine, as can be realized by comparing for instance welds illustrated in Fig. 6 and Fig. 7 with welds done with similar parameters in a FSW machine, see [17]. This difference can be explained by the additional heat supplied by the tool shoulder to the welds.

4.2. Axial force

As shown above, high rotational speed generates more heat by friction and thus promotes mixing of material and adhesion to base material. If rotational speed is low the axial force is a key factor to do good welds. Fig. 10(a) shows that all welds performed with lower rotational speed (1000 and 1250 (rpm)) practically have increase in tensile strength with the increase in axial force. This effect is more visible between the welds performed at 1 (kN) and 1.5 (kN). Considering just the welds performed at high rotational speed (R1500T50, R1500T100 and R1500T200), Fig. 10(a), it appears that its tensile strength does not have significant change. These results are in good agreement with those presented by Mendes et al. [17] which demonstrate that the axial force does not cause any effect in tensile strength of welds performed with high rotational speed (1500 (rpm)).

In the current study, the strain at break of the robotic welds increases with increase of axial force, comparing the welds performed at 1 (kN) with the welds performed at 1.5 and 2 (kN). The two latter welds present clearly higher strain values than the former weld. In the previous study, the welds done using similar welding conditions (R1500T100F0.75, R1500T100F2.25) present similar trend and strain values comparable to those welds performed in the robotic system, R1500T100F1 and R1500T100F2, respectively.

4.3. Rotational speed

The effect of the tool rotational speed on morphology of robotic welds is mirrored in a decrease of the number and size of defects with increasing rotational speed, as shown above in R1000T100F1, R1250T100F1 and R1500T100F1. The welds performed in the FSW machine with similar parameters (R1000T100F0.75, R1250T100F0.75 and R1500T100F0.75) present exactly the same effect, i.e. the quantity and size of weld defects decrease with increase in rotational speed. The effect of the rotational speed on mechanical properties (tensile strength and strain at break) of the welds done in both systems (robotic system and FSW machine) is similar, i.e., mechanical properties increase with increasing rotational speed, as shown in Table 3. The tensile strength and strain increase as the defects in the weld decrease. It is clearly visible that the welds performed in the robotic system present better crown surface (Fig. 6) and morphology through the thickness direction (Fig. 7) than the welds performed in the FSW machine. The same effect is confirmed by the mechanical properties of the welds shown in Table 3. This effect may be explained by supplying external heat to the weld and by the slight difference of the axial force parameter which was used in the welds production.

4.4. Traverse speed

It is difficult to establish a particular relation between traverse speed and the mechanical properties of the welds. By the analysis of Fig. 12(a), it is probably that in welding conditions less favourable, i.e. where less heat is generated due to low values of rotational speed or axial force, the increase in traverse speed provides improvement of the tensile strength of the welds. However, the tensile strength of these welds is in general low. On the other hand, in welding conditions where more heat is generated, it seems that the welds do not suffer any change or suffer a small decrease in tensile strength with increasing traverse speed. The strain property of the welds is clearly improved with decrease of the traverse speed. In the previous study, where the welds were performed in the FSW machine, just a set of welds was taken into consideration (R1250T50F3.75, R1250T100F2 and R1250T200F3.25). It was verified that there was no significant effect on the mechanical properties of the welds with the parameter traverse speed. This was likely because all of these welds were performed at relatively high axial force which, as demonstrated above, improves weld quality.

During the welding process it was verified that low traverse speed leads to overheating or keeping of tool temperature which dismisses external heating. This phenomenon was verified in welds performed at low traverse speed (50 (mm/min)) and high axial force (1.5 or 2 (kN)) and rotational speed (1250 or 1500 (rpm)). Since this heat flux flows through the FSW tool to weld surface, as described above, it is plausible to state that traverse speed has a strong influence on temperature reached on weld crown surface. The study carried out by Bagheri et al. [15] claims that lower traverse speed leads to weld with higher tensile strength. This suggests that lower traverse speed leads to a scenario in which the shoulder and the pin heat the welding zone for a longer time, providing more heat to weld. However, Bagheri et al. [15] took into account welds which have been performed at very low traverse speeds. The welds which presented a meaningful improvement of tensile strength property were performed at 20 (mm/min). From an industrial point of view, so low traverse speed values are considered unattractive and impracticable. By this reason traverse speeds lower than 50 (mm/min) are despised. Nevertheless, comparing the results obtained in the current study with results reported by Bagheri et al. [15], it can be stated that just very low traverse speeds can really improve tensile strength of weld.

4.5. Overview

In general, the weld results performed in the robotic system are similar to the weld results performed in the FSW machine [17], where it was not used external heating. The mechanical properties of the welds performed in the robotic system display the same evolution tendencies as the welds performed in the FSW machine when the welding parameters (axial force, rotational speed and traverse speed) are changed. However, there are slightly differences between the welds performed in the robotic system and in the FSW machine that can be justified by supplying external heating to welds. This suggests that the welding parameter temperature of the FSW tool influences weld quality, mainly the weld crown surface.

5. Conclusions

The aim of the present research is to study the effect of the axial force, tool rotational and traverse speeds as well as the tool temperature, on the quality of welds carried out by FSW on ABS plates using a robotic system and a stationary shoulder tool. Furthermore, results are compared with welds performed in a FSW machine [17]. Based on the experimental results and discussion, the following conclusions can be drawn:

- It is feasible to produce good quality welds in a robotic FSW system;

- A tool temperature of 115 (°C) improves weld quality, specially the weld crown surface;
- High axial force promotes the squeeze of the molten polymeric material, preventing introduction of air into the weld and helps cooling of the weld, avoiding shrinkage and voids formation.
- High axial force improves tensile strength and strain of welds;
- The rotational speed is primarily responsible for heat generation, promoting adequate plasticizing and mixing the polymer;
- High tool rotational speed improves tensile strength and strain of welds;
- Welds free of defects present the same hardness as base material;
- To prevent lack of heat or overheating of the tool the R/T ratio must range between 10 and 20;
- A quality weld is obtained for tool temperature of 115 (°C), axial force higher than 1.5 (kN), rotational speed higher than 1250 (rpm) and low traverse speed (ranging between 50 and 100 (mm/min));
- The welds produced in the robotic system present similar or better appearance and mechanical properties than the welds produced in the FSW machine;

Acknowledgements

This research is supported by FEDER funds through the program COMPETE (*Programa Operacional Factores de Competitividade*), under the project CENTRO-07-0224-FEDER-002001(MT4MOBI) and by national funds through FCT (*Fundação para a Ciência e a Tecnologia*) under the project PEst-C/EME/UI0285/2013 and the grant no. SFRH/BD/62485/2009. The authors are grateful to ThyssenKrupp Portugal - Aços e Serviços SA for the heat treatment of the FSW tools and Yaskawa Ibérica for the equipment and support provided.

References

- [1] Strand S. Joining plastics - can friction stir welding compete? Proc. Electr. Insul. Conf. Electr. Manuf. Coil Wind. Technol. Conf. (Cat. No.03CH37480), IEEE; 2003, p. 321–6.
- [2] Nelson T. W, Sorenson CD, Johns CJ. Friction stir welding of polymeric materials. US 6811632 B2, 2004.
- [3] Strand S. Effects of friction stir welding on polymer microstructure. Brigham Young University, 2004.
- [4] Kiss Z, Czigány T. Applicability of friction stir welding in polymeric materials. Period Polytech Mech Eng 2007;51:15.

- [5] Scialpi A, Troughton M, Andrews S, De Filippis LAC. In-line reciprocating friction stir welding of plastics. *Join Plast von Kunststoffen* 2007;1:42–51.
- [6] Scialpi A, Troughton M, Andrews S, De Filippis LAC. Viblade™: friction stir welding for plastics. *Weld Int* 2009;23:846–55.
- [7] Aydin M. Effects of Welding Parameters and Pre-Heating on the Friction Stir Welding of UHMW-Polyethylene. *Polym Plast Technol Eng* 2010;49:595–601.
- [8] Bozkurt Y. The optimization of friction stir welding process parameters to achieve maximum tensile strength in polyethylene sheets. *Mater Des* 2012;35:440–5.
- [9] Payganeh GH, Arab NBM, Asl YD, Ghasemi FA, Boroujeni MS. Effects of friction stir welding process parameters on appearance and strength of polypropylene composite welds. *Int J Phys Sci* 2011;6:4595–601.
- [10] Arici A, Sinmazçelyk T. Effects of double passes of the tool on friction stir welding of polyethylene. *J Mater Sci* 2005;40:3313–6.
- [11] Panneerselvam K, Lenin K. Investigation on Effect of Tool Forces and Joint Defects During FSW of Polypropylene Plate. *Procedia Eng* 2012;38:3927–40.
- [12] Panneerselvam K, Lenin K. Joining of Nylon 6 plate by friction stir welding process using threaded pin profile. *Mater Des* 2014;53:302–7.
- [13] Kiss Z, Czigány T. Effect of welding parameters on the heat affected zone and the mechanical properties of friction stir welded poly(ethylene-terephthalate-glycol). *J Appl Polym Sci* 2012;125:2231–8.
- [14] Kiss Z, Czigány T. Microscopic analysis of the morphology of seams in friction stir welded polypropylene. *Express Polym Lett* 2012;6:54–62.
- [15] Bagheri A, Azdast T, Doniavi A. An experimental study on mechanical properties of friction stir welded ABS sheets. *Mater Des* 2013;43:402–9.
- [16] Pirizadeh M, Azdast T, Rash Ahmadi S, Mamaghani Shishavan S, Bagheri A. Friction stir welding of thermoplastics using a newly designed tool. *Mater Des* 2014;54:342–7.
- [17] Mendes N, Loureiro A, Martins C, Neto P, Pires JN. Effect of friction stir welding parameters on morphology and strength of acrylonitrile butadiene styrene plate welds. *Mater Des* 2014;58:457–64.
- [18] Schneider U, Drust M, Ansaloni M, Lehmann C, Pellicciari M, Leali F, et al. Improving robotic machining accuracy through experimental error investigation and modular compensation. *Int J Adv Manuf Technol* 2014.
- [19] Leali F, Vergnano A, Pini F, Pellicciari M, Berselli G. A workcell calibration method for enhancing accuracy in robot machining of aerospace parts. *Int J Adv Manuf Technol* 2014.
- [20] Mendes N, Neto P, Simão MA, Loureiro A, Pires JN. A novel friction stir welding robotic platform: welding polymeric materials. *Int J Adv Manuf Technol* 2014.
- [21] Mendes N, Neto P, Pires JN, Loureiro A. An optimal fuzzy-PI force/motion controller to increase industrial robot autonomy. *Int J Adv Manuf Technol* 2013;68:435–41.

- [22] Poggio C, Lombardini M, Gaviati S, Chiesa M. Evaluation of Vickers hardness and depth of cure of six composite resins photo-activated with different polymerization modes. *J Conserv Dent* 2012;15:237–41.
- [23] Nandan R, Roy GG, Lienert TJ, Debroy T. Three-dimensional heat and material flow during friction stir welding of mild steel. *Acta Mater* 2007;55:883–95.
- [24] Heurtier P, Jones MJ, Desrayaud C, Driver JH, Montheillet F, Allehaux D. Mechanical and thermal modelling of Friction Stir Welding. *J Mater Process Technol* 2006;171:348–57.
- [25] Neto DM, Neto P. Numerical modeling of friction stir welding process: a literature review. *Int J Adv Manuf Technol* 2012;65:115–26.
- [26] Oliveira PHF, Amancio-Filho ST, dos Santos JF, Hage E. Preliminary study on the feasibility of friction spot welding in PMMA. *Mater Lett* 2010;64:2098–101.
- [27] Sorensen CD, Nelson TW, Strand S, Johns C, Christensen J. Joining of Thermoplastics with Friction Stir Welding. *Tech. Pap. Annu. Tech. Conf. Plast. Eng. Incorporated (ANTEC 2001)*, 2001, p. 1246–50.
- [28] Frassine R, Rink M, Leggio A, Pavan A. Experimental analysis of viscoelastic criteria for crack initiation and growth in polymers. *Int J Fract* 1996;81:55–75.

Figure captions

Fig. 1. Representation of the FSW process.

Fig. 2. FSW tool with long stationary shoulder and conical threaded pin.

Fig. 3. Effect of temperature on the morphology of the weld crown: (a) R1500T60F1 low temperature: 90 (°C), (b) R1000T200F1 recommended temperature: 115 (°C) and (c) R1500T50F1 excessive temperature: 130 (°C).

Fig. 4. Effect of axial force on the morphology of the weld crown: (a) R1000T50F1, (b) R1000T50F1.5 and (c) R1000T50F2 (AS – advancing side; RS – retreating side).

Fig. 5. Micrographs of welds performed with increasing axial force: (a) R1000T50F1, (b) R1000T50F1.5 and (c) R1000T50F2 (AS – advancing side; RS – retreating side).

Fig. 6. Effect of rotational speed on the morphology of the weld crown: (a) R1000T100F1, (b) R1250T100F1 and (c) R1500T100F1 (AS – advancing side; RS – retreating side).

Fig. 7. Micrographs of welds performed with increasing rotational speed: (a) R1000T100F1, (b) R1250T100F1 and (c) R1500T100F1 (AS – advancing side; RS – retreating side).

Fig. 8. Effect of traverse speed on the morphology of the weld crown: (a) R1250T50F2, (b) R1250T100F2 and (c) R1250T200F2 (AS – advancing side; RS – retreating side).

Fig. 9. Micrographs of welds performed with increasing traverse speed: (a) R1250T50F2, (b) R1250T100F2 and (c) R1250T200F2 (AS – advancing side; RS – retreating side).

Fig. 10. Effect of axial force on: (a) the tensile strength; (b) the strain at break of the welds.

Fig. 11. Effect of rotational speed on: (a) the tensile strength; (b) the strain at break of the welds.

Fig. 12. Effect of traverse speed on: (a) the tensile strength; (b) the strain of the welds.

Fig. 13. Hardness profile of the weld R1500T100F200.

Table captions

Table 1 Main properties of ABS material.

Table 2 Tensile strength efficiency (%) and strain of welds (%) produced in the robotic system.

Table 3 Tensile strength efficiency (%) and strain of welds (%) produced in the robotic system and in the FSW machine.

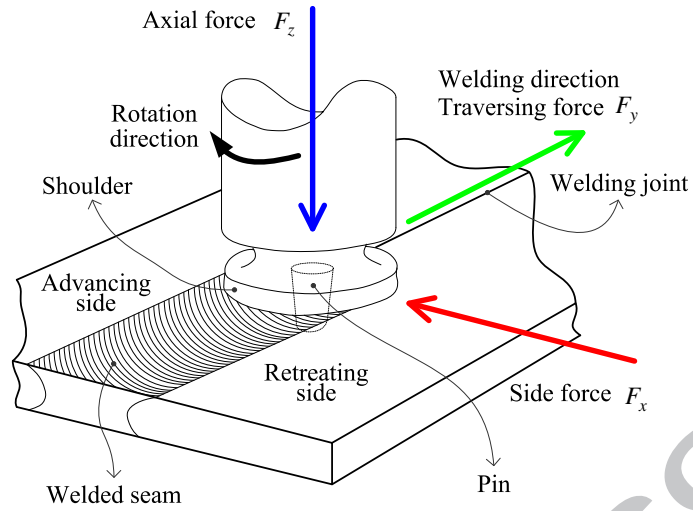


Fig. 1. Representation of the FSW process.

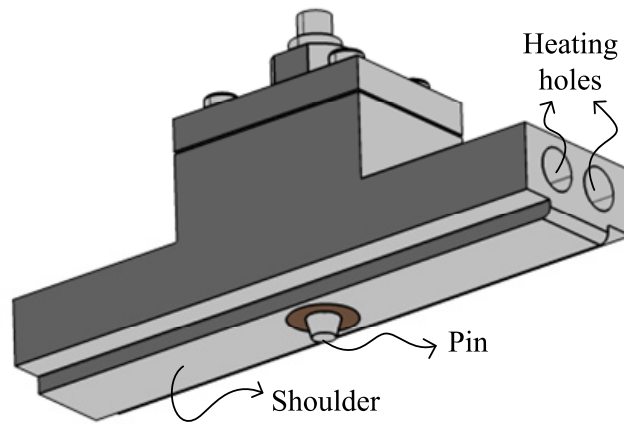


Fig. 2. FSW tool with long stationary shoulder and conical threaded pin.

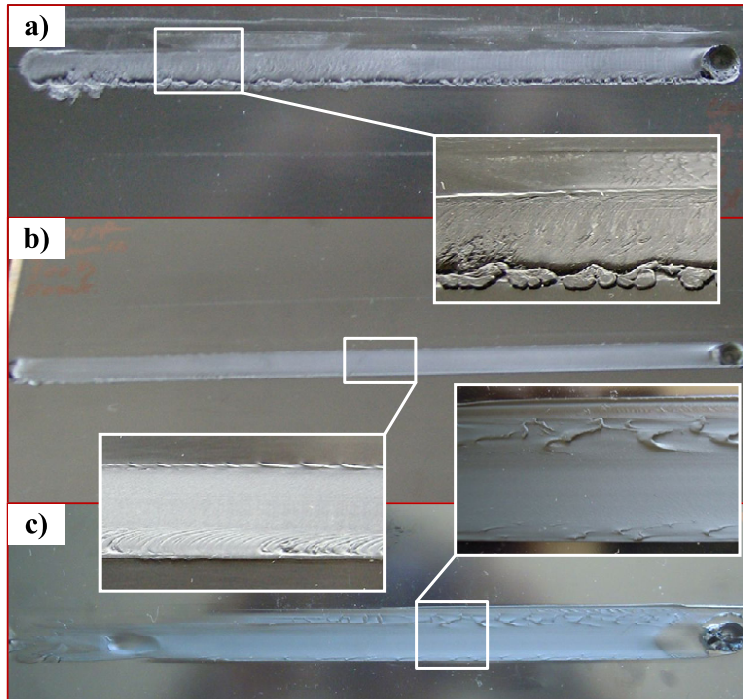


Fig. 3. Effect of temperature on the morphology of the weld crown: (a) R1500T60F1 low temperature: 90 (°C), (b) R1000T200F1 recommended temperature: 115 (°C) and (c) R1500T50F1 excessive temperature: 130 (°C).

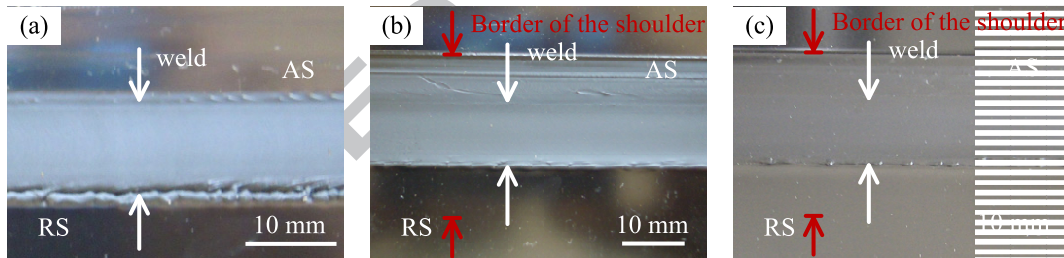


Fig. 4. Effect of axial force on the morphology of the weld crown: (a) R1000T50F1, (b) R1000T50F1.5 and (c) R1000T50F2 (AS – advancing side; RS – retreating side).

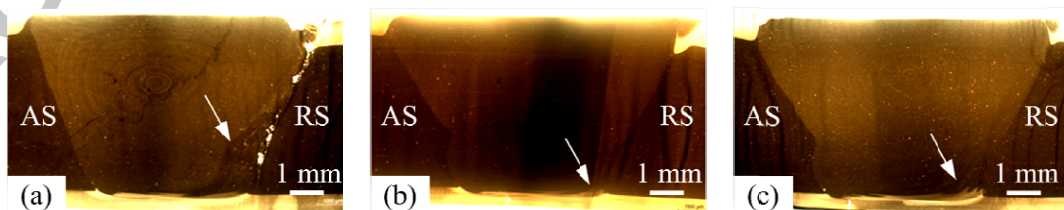


Fig. 5. Micrographs of welds performed with increasing axial force: (a) R1000T50F1, (b) R1000T50F1.5 and (c) R1000T50F2 (AS – advancing side; RS – retreating side).

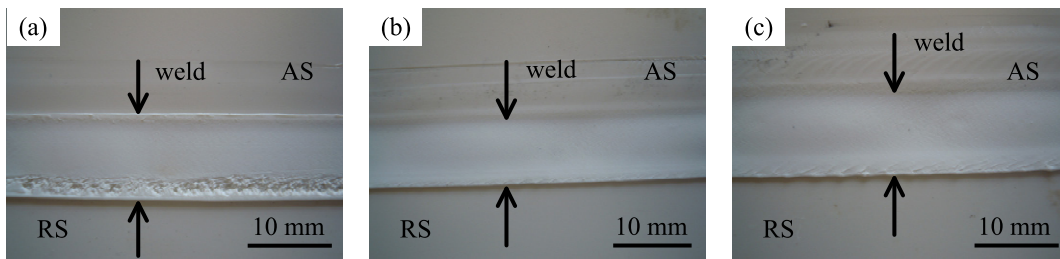


Fig. 6. Effect of rotational speed on the morphology of the weld crown: (a) R1000T100F1, (b) R1250T100F1 and (c) R1500T100F1 (AS – advancing side; RS – retreating side).

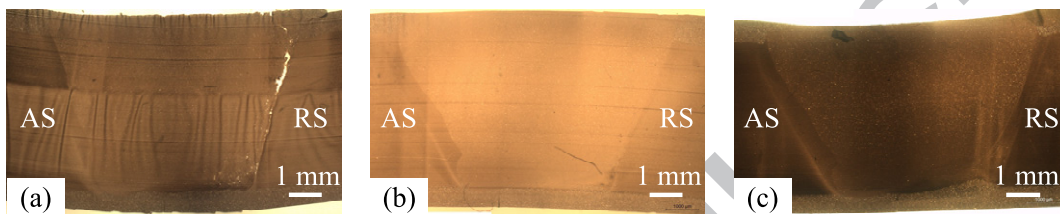


Fig. 7. Micrographs of welds performed with increasing rotational speed: (a) R1000T100F1, (b) R1250T100F1 and (c) R1500T100F1 (AS – advancing side; RS – retreating side).

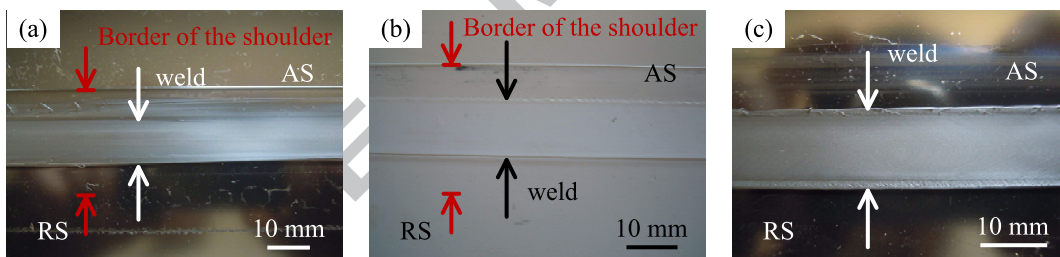


Fig. 8. Effect of traverse speed on the morphology of the weld crown: (a) R1250T50F2, (b) R1250T100F2 and (c) R1250T200F2 (AS – advancing side; RS – retreating side).

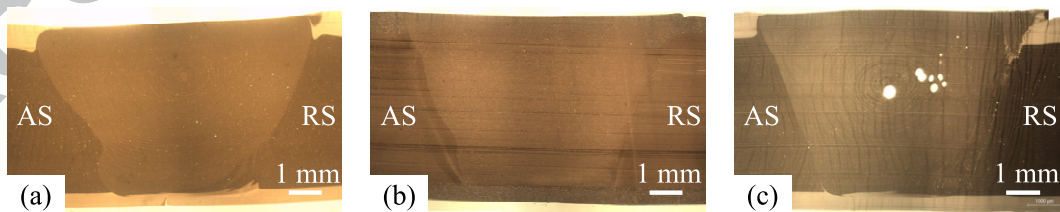


Fig. 9. Micrographs of welds performed with increasing traverse speed: (a) R1250T50F2, (b) R1250T100F2 and (c) R1250T200F2 (AS – advancing side; RS – retreating side).

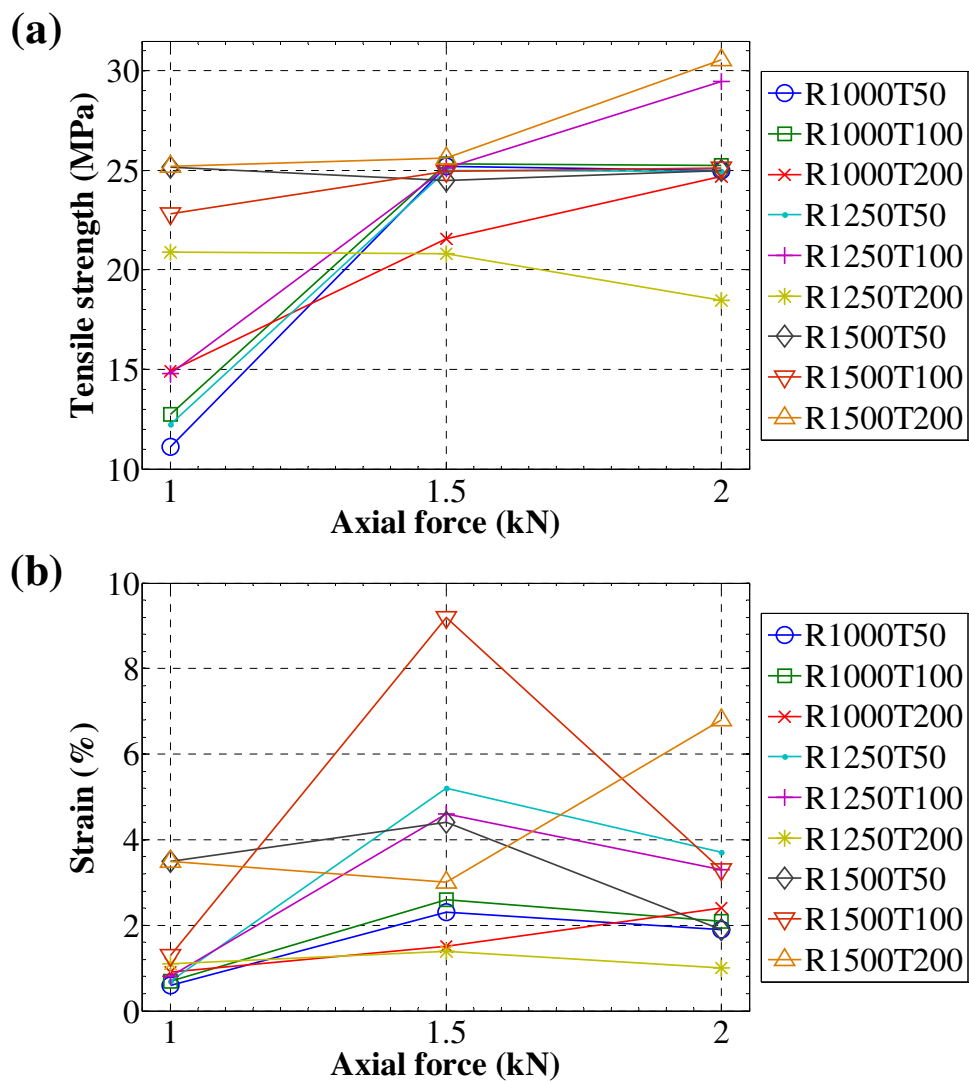


Fig. 10. Effect of axial force on: (a) the tensile strength; (b) the strain at break of the welds.

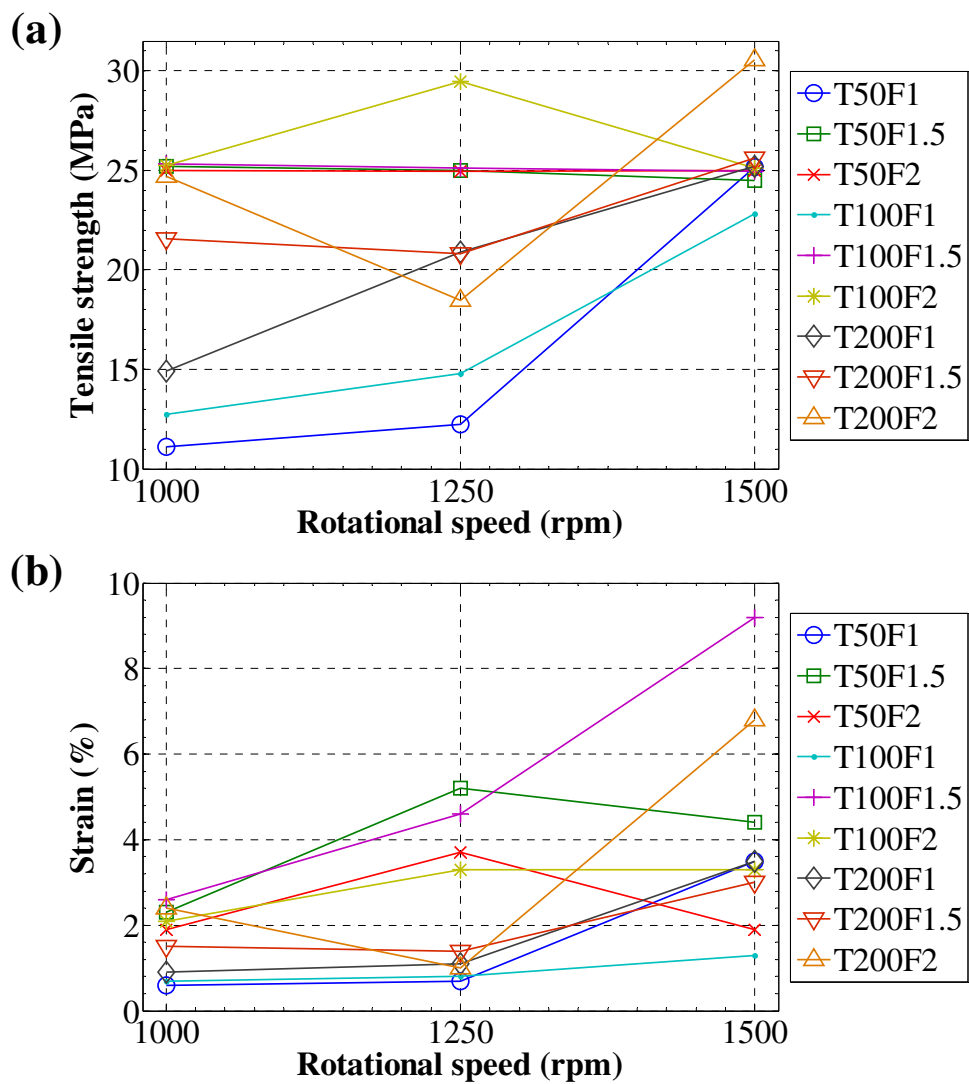


Fig. 11. Effect of rotational speed on: (a) the tensile strength; (b) the strain at break of the welds.

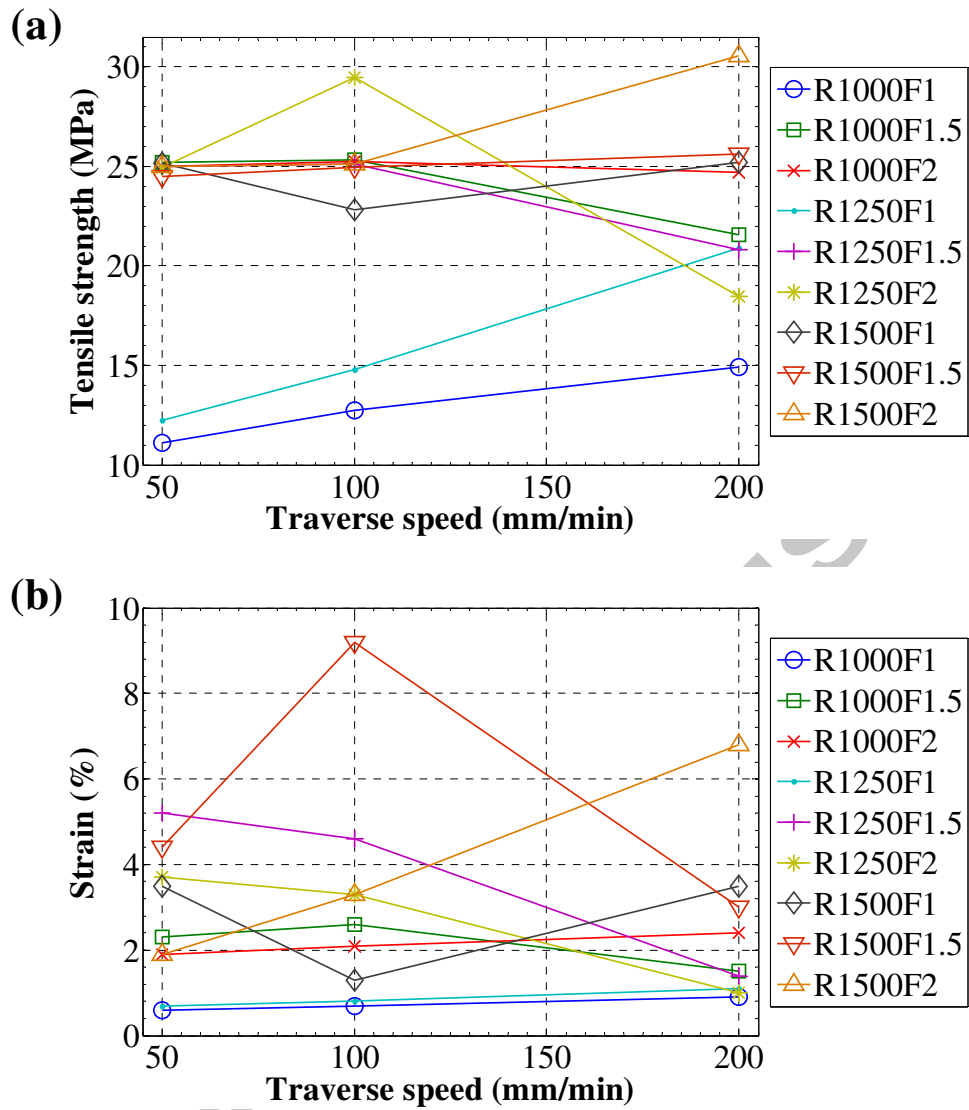


Fig. 12. Effect of traverse speed on: (a) the tensile strength; (b) the strain of the welds.

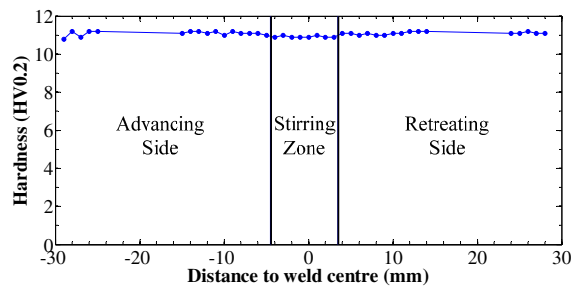


Fig. 13. Hardness profile of the weld R1500T100F200.

Table 1

Main properties of ABS material.

| Density (g/cm ³) | Tensile strength (MPa) | Strain at break (%) | Hardness (HV0.2) | Glass transition temperature (°C) |
|------------------------------|------------------------|---------------------|------------------|-----------------------------------|
| 1.04 | 40.5 | 50 | 11 | 105 |

Table 2

Tensile strength efficiency (%) and strain of welds (%) produced in the robotic system.

| T (mm/min) ↓ | R (rpm) → | 1000 | | 1250 | | 1500 | |
|--------------|-----------|-------------------------|------------|-------------------------|------------|-------------------------|------------|
| | | Strength efficiency (%) | Strain (%) | Strength efficiency (%) | Strain (%) | Strength efficiency (%) | Strain (%) |
| 50 | 1 | 27.4 | 0.6 | 30.2 | 0.7 | 62.2 | 3.5 |
| | 1.5 | 62.2 | 2.3 | 61.7 | 5.2 | 60.5 | 4.4 |
| | 2 | 61.7 | 1.9 | 61.6 | 3.7 | 61.7 | 1.9 |
| 100 | 1 | 31.5 | 0.7 | 36.5 | 0.8 | 56.3 | 1.3 |
| | 1.5 | 62.5 | 2.6 | 62.0 | 4.6 | 61.6 | 9.2 |
| | 2 | 62.3 | 2.1 | 72.8 | 3.3 | 62.0 | 3.3 |
| 200 | 1 | 36.8 | 0.9 | 51.6 | 1.1 | 62.2 | 3.5 |
| | 1.5 | 53.3 | 1.5 | 51.4 | 1.4 | 63.3 | 3.0 |
| | 2 | 61.0 | 2.4 | 45.6 | 1.0 | 75.5 | 6.8 |

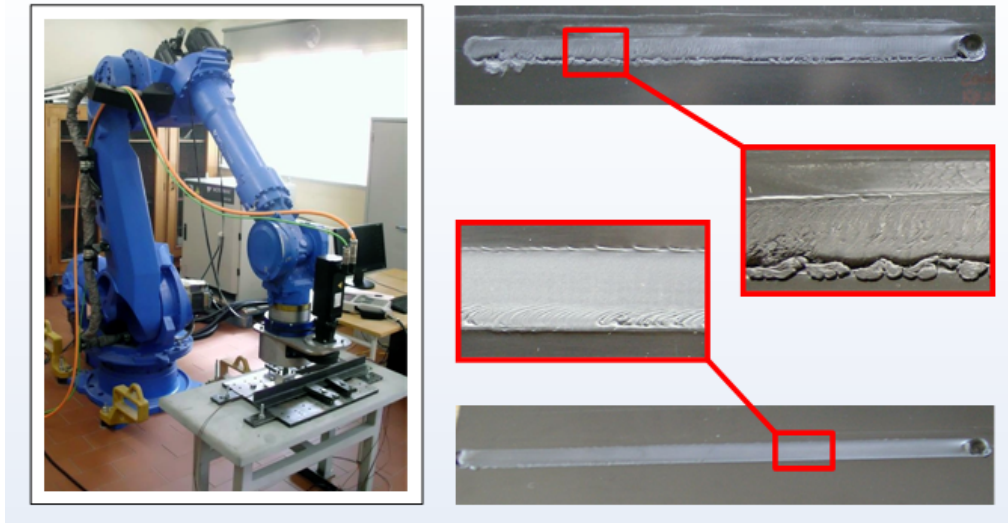
Table 3

Tensile strength efficiency (%) and strain of welds (%) produced in the robotic system and in the FSW machine.

| Weld | R1000T100F... | | R1250T100F... | | R1500T100F... | |
|-----------------|-------------------------|------------|-------------------------|------------|-------------------------|------------|
| | Strength efficiency (%) | Strain (%) | Strength efficiency (%) | Strain (%) | Strength efficiency (%) | Strain (%) |
| Robotic (F1) | 31.5 | 0.7 | 36.5 | 0.8 | 56.3 | 1.3 |
| Machine (F0.75) | 31.0 | 0.5 | 35.0 | 0.8 | 62.0 | 1.2 |

Graphical abstract

Robotic Friction Stir Welding of ABS



ACCEPTED

IPT

Research highlights:

- Robotic friction stir welding of acrylonitrile butadiene styrene;
- The welds produced in a robotic system and in a FSW machine present similar quality;
- Influence of friction stir welding parameters on the quality of welds;
- Axial force and tool rotational speed are the most influential in the process;
- Axial force contributes to material mixing and prevents the formation of cavities.

ACCEPTED MANUSCRIPT